Corrugated QWIP Developments for Tactical Infrared Imaging

David P. Forrai[a], Kwong-Kit Choi[b], John W. Devitt[a]
[a]L-3 Communications Cincinnati Electronics, 7500 Innovation Way, Mason, OH, USA 45040
[b]U.S. Army Research Laboratory, 2800 Powder Mill Road, Adelphi, MD 20783

ABSTRACT

The corrugated quantum well infrared detector (C-QWIP) offers improvements to quantum efficiency and spectral bandwidth compared to current commercial QWIPs. In addition to improved performance, the C-QWIP also uses manufacturing processes that are mature and low cost. Thus, very large format focal plane arrays (FPAs) can be fabricated with high yield. There are two applications where the C-QWIP can provide cost effective solutions. The first is very large format long-wave infrared (LWIR) sensors. Most very large format FPAs operate in the mid-wave infrared (MWIR). The MWIR band has significantly lower flux than LWIR, therefore in situations where the backgrounds are cold or there is potential motion blur, the LWIR C-QWIP offers better performance. The second application is two-color registered high-resolution wide area imagery. ARL and CE have been developing both C-QWIP detectors and read-out integrated circuits to support these needs. This paper describes the progress we've made in developing high conversion efficiency LWIR C-QWIP FPAs and MWIR/LWIR two-color FPAs and our path forward to multi-megapixel C-QWIP FPAs and sensors.

INTRODUCTION

L-3 Communications Cincinnati Electronics (CE) and the Army Research Laboratory (ARL) have been collaborating on the development of large format focal plane arrays (FPAs) using the corrugated quantum well infrared photodetector (C-QWIP). This technology shows promise to overcome many obstacles which so far have prevented QWIP-based sensors from satisfying the requirements for tactical infrared imaging systems.

The main advantage of QWIPs for tactical applications is cost. QWIPs use alternating layers of wide band gap gallium arsenide (GaAs), indium gallium arsenide (InGaAs), and aluminum gallium arsenide (AlGaAs) epitaxially grown GaAs substrates. GaAs epitaxy is used in a broad range of electron devices; hence there are a variety of commercial vendors capable of producing the QWIP wafers with high uniformity. Wafers sizes up to 150 mm (6 inches) are common today and sizes up to 200 mm (8 inches) are likely to become available in the near future. Since the QWIP is fabricated using wide band gap materials, it is not plagued by ineffective passivation that impacts direct band gap infrared (IR) materials. These attributes allow for low cost, highly uniform wafers and the fabrication of multiple die of large format FPAs on a single wafer that leads to high yield.

A QWIP is a photoconductor. Unlike a photodiode, it does not contain an internal electric field. Thus an external electric field must be applied across the detector to induce current flow. With the incident optical flux, photoelectrons are generated in the conduction band. Thus, the conductance of the detector changes with incident flux. Since the detector has a finite conductance, there will always be a dark current associate with the photocurrent. For effective imaging, the dark current must be significantly less than the photocurrent.

The electrons have a fixed transit time across the detector, which is a function of the material and the device thickness. The photoelectrons have a recombination lifetime. In the QWIP, the recombination lifetime is usually shorter than the transit time. Thus QWIPs exhibit a noiseless photoconductive gain less than 1. Although the photoconductive gain does not affect noise when operating at or below the background limit, it can lengthen the integration time, which can be undesirable in a tactical application.

The QWIP relies on an intrasubband transition of an electron within the conduction band. The electrons are trapped in a quantum well (QW) and elevated above the surrounding barrier by photon absorption. When a photon is absorbed and an electron elevated above the barrier, the applied electric field sweeps the electron across the detector and a charge remains in the well for future recombination. In low flux or high f/# applications, this remaining charge can reduce the

Infrared Systems and Photoelectronic Technology II, edited by Randolph E. Longshore, Ashok K. Sood, Eustace L. Dereniak, John P. Hartke, Proc. of SPIE Vol. 6660, 666010, (2007)
0277-786X/07/$18 · doi: 10.1117/12.740311

bandwidth of the detector. This does not impact most terrestrial tactical applications, however it represents a limitation for QWIP FPAs.

For photon absorption to occur in the QWIP, the electric field of the incident light must be perpendicular to the quantum wells. This is orthogonal to the direction of incidence on the detector. Hence, the critical design parameter in the QWIP structure is the optical element that turns the incident light in the correct direction such that absorption quantum efficiency (QE) is maximized.

In the following sections, we will describe the C-QWIP, some potential tactical applications for the C-QWIP, and how we intend to reduce the limitations imposed by dark current, photoconductive gain, quantum efficiency, and low flux in order to meet the needs of those tactical applications.

1. DESCRIPTION OF THE C-QWIP

The C-QWIP incorporates micro-mirrors in the detector structure to turn the incident light in the horizontal direction. Figure 1 illustrates the basic structure. The IR light is incident through the GaAs substrate. It propagates normally through the QW layers unabsorbed until it reaches the tilted micro-mirrors. It reflects off the micro-mirrors and propagates horizontally through the QW layers where the transverse magnetic (TM) portion of the incident light is absorbed. Any remaining light is reflected off the second mirror and out of the detector.

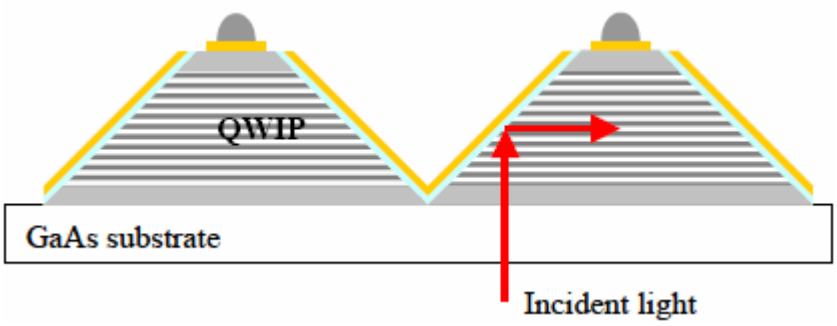

Figure 1: Illustration of the C-QWIP detector structure.

The advantage of the C-QWIP design is that the micro-mirrors are inherently highly reflective over a wide bandwidth. This allows the C-QWIP to support narrow band, wide band, and dual-band detectors without any changes to the wafer processing. The C-QWIP has a theoretical maximum absorption QE of 50%. Due to the varying absorption path length across the detector, and the fill factor limitation imposed by the bump platform, the practical limit for peak QE in the current quasi two-dimensional detector structure is around 35%. The C-QWIP can readily attain a band average absorption QE of over 20%. Figure 2 plots the spectral response in arbitrary units of narrow and wide band FPAs fabricated by ARL and CE.

Another advantage of the C-QWIP is the straightforward processing steps required. A QWIP wafer can be processed into C-QWIP arrays with as few as 5 processing steps. These processes involve common equipment, such as UV photolithography, wet and dry etching, and metal and dielectric evaporation or sputtering. Thus the C-QWIP FPA is well suited for volume production and could be ramped up with a relatively small manufacturing technology investment.

The most cost effective IR material system today is indium antimonide (InSb). InSb is available in wafer sizes up to 100 mm with high material quality and uniformity. The C-QWIP is the only material system that can match, or even beat, the per FPA cost of InSb. Given the tunability of the QW spectral response over most of the IR band and longer wavelengths, C-QWIP FPAs potentially satisfy a wide variety of IR imaging needs.

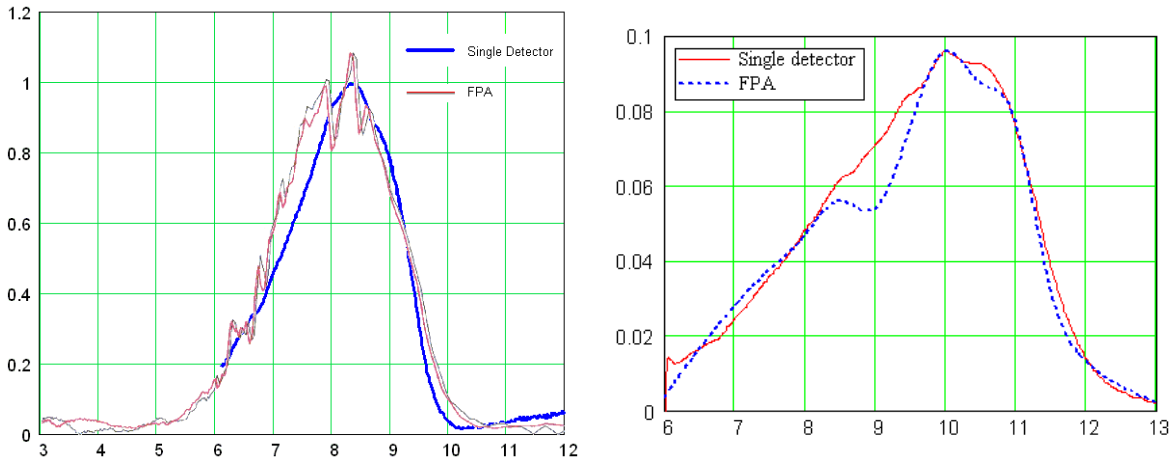

Figure 2: Narrow (left) and wide (right) band LWIR responses of C-QWIP FPAs fabricated.

2. TACTICAL LWIR FPAS

Tactical systems have a need for large format, LWIR FPAs. The two applications needing 1K or greater formats are pilotage and persistent surveillance. Current systems rely on large format MWIR sensors. MWIR sensors offer advantages in terms of range and resolution but disadvantages in terms of motion blur and cold background performance. To minimize motion blur, integration times of at most 2 milliseconds, and preferably less than 1 millisecond, are needed. In cold weather, MWIR sensitivity degrades due to the rapidly decreasing background flux. It is difficult to maintain a sensor sensitivity in the 20 mK range much below 0° C. LWIR performs much better than MWIR in cold weather, as illustrated in Figure 3.

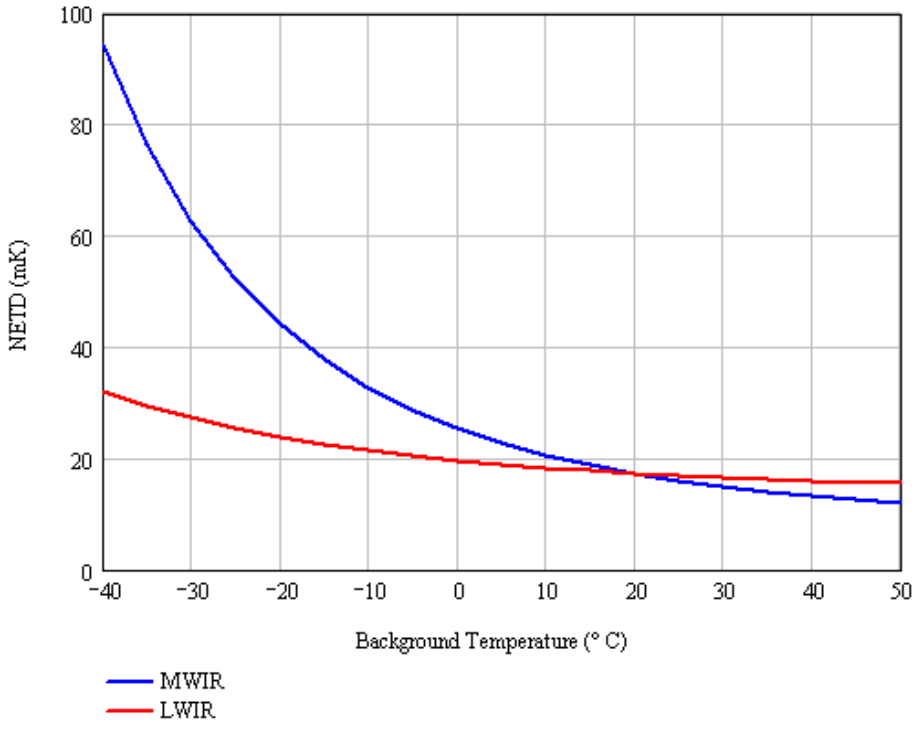

Figure 3: Calculation of NETD based on background temperature for a MWIR and LWIR C-QWIP detector.

The degradation of the MWIR detector in Figure 3 is less a function of the detector and more a function of the background flux. Clearly the LWIR C-QWIP shows advantage in cold weather performance, the question that remains is whether the C-QWIP detector can meet the integration time requirement.

In an earlier paper[1], we highlighted the figures of merit for a C-QWIP FPA. Table 1 maps detector parameters from those figures of merit to system level parameters. Note that in many cases, the choice is contradictory. For instance, to minimize integration time, we need to maximize the QE-photoconductive gain product. Increasing the thickness of the active QW region increases the QE, but that decreases the photoconductive gain. The second system parameter, minimizing NETD, guides us to maximize QE over maximizing photoconductive gain. This is intuitive since maximizing QE in a detector is always best. Another example is with the operating temperature. Photocurrent increases with increasing bandwidth. But since the LWIR atmospheric window starts to open after 7.5 μm, the only way to increase bandwidth is to lengthen the cut-off wavelength. But lengthening the cut-off wavelength increases dark current. These parameters form a complex trade space of parameters that are often conflicting. To try and satisfy tactical LWIR applications, we established goals to maximize QE through doping and maximizing the number of quantum wells, fix the cut-off wavelength around 9 μm, and use InGaAs QWs to increase photoconductive gain. The remaining paragraphs in this section will describe the progress we've made towards these goals.

Table 1: Translation of system parameters to C-QWIP characteristics.

System Parameter to Improve	Detector Parameter to Change	Method of Changing Detector Parameter in the C-QWIP
Minimize integration time	Increase QE × photoconductive gain	Increase QE through better optical coupling, thicker active region, and higher doping
		Increase photoconductive gain by using a thinner active region and a higher detector bias
Minimize NETD	Increase QE	Increase QE through better optical coupling, thicker active region, and higher doping
Maximize operating temperature	Increase I_{photo}/I_{dark}	Increase I_{photo} by increasing QE and increasing bandwidth
		Decrease I_{dark} with reduced doping, a shorter cut-off wavelength, and lower detector bias.

2.1. LC5 FPAs

We prefix wafers designed for C-QWIP pixels like that shown in Figure 1 with "LC" (which abbreviates "large corrugation"). A large corrugation means that each pixel has one pair of micro-mirrors. Our first attempt at a tactical wafer design was LC5. Our initial goals were modest due to limitations on detector bias imposed by the read-out integrated circuit (ROIC) and by the bias supply in the camera. Therefore, some compromise was made in the number of quantum wells. Still, the expected peak QE was around 25% and the photoconductive gain around 0.3. This was expected to attain a 50% well fill for integration times less than 5 milliseconds against a 20° C background.

Our material growth calibration runs yielded test devices with a sharp 9 μm cut-off as shown in the upper right-hand plot of Figure 4. However, due to variations in the growth process that were unknown at the time, the actual spectrum of the FPAs had a 10 μm cut-off, as shown in the lower right-hand plot of Figure 4. The result of this longer and less sharp cut-off was that our operating temperature was approximately 10K colder than what we desired. It should be noted that during our wafer calibration runs, a wafer lot was grown that exhibited the measured spectrum shown in the upper left-hand plot of Figure 4. This lot was rejected due to the short cut-off wavelength of the test device. We now expect the wafer to have the spectrum shown in the lower left-hand plot of Figure 4, so we are fabricating one wafer from this lot into FPAs for evaluation. These wafers may respond similarly to the accepted LC5 lot but have an operating temperature at least 5K higher than the current FPAs due to the shorter cut-off wavelength.

The LC5 material was fabricated into 1K×1K FPAs with a 25 μm pixel pitch. Most FPAs fabricated had operabilities over 99.5%. This highlights both the material uniformity and manufacturability of the C-QWIP FPAs. This high yield on a small development run is indicative of high yields and low FPA costs when transitioned to production.

The measured photoconductive gain was around 0.17. The peak quantum efficiency was much higher. It measured around 35%. Thus, in a camera configuration (lens and 8-10 µm cold filter) we were able to achieve 50% well fill in 3.8 millisecond with a NETD of 22 mK. Aside from operating temperature, the LC5 FPA run was a success.

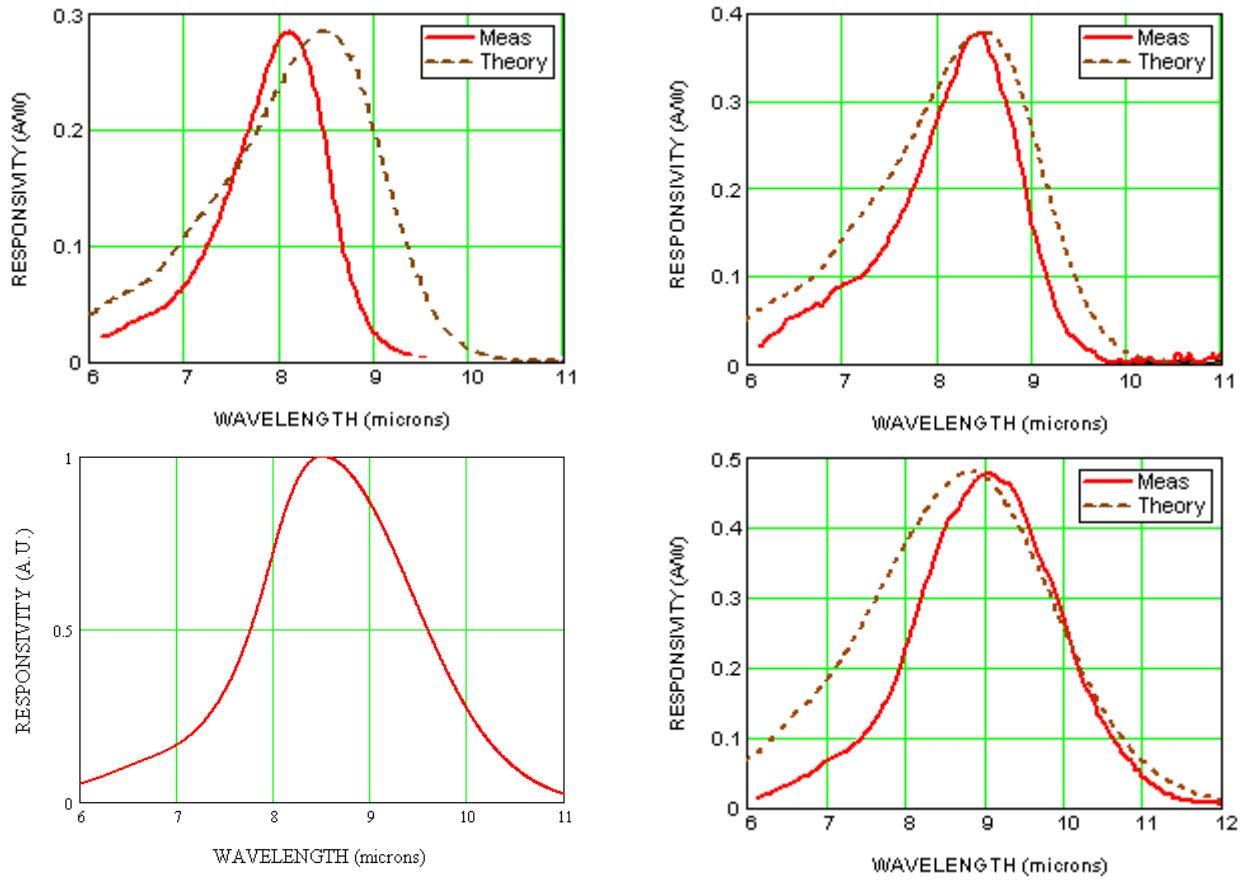

Figure 4: Staring from the upper left plot going clockwise, the spectrum from the first wafer lot test detector (rejected), the second wafer lot test detector (accepted), the delivered LC5 wafers, and the anticipated true spectrum of the first wafer lot.

2.2. LC6 FPAs

Given the need for higher bias and two-color FPA support, CE designed and fabricated a new ROIC. This ROIC is designed to accept bias of either polarity up to 10 volts. In addition to supporting the higher bias, we implemented both dark charge skimming and programmable well size. The dark charge skimming may allow us to operate at elevated operating temperatures as the FPA will have the ability to maintain dynamic range with larger dark current. The programmable well size allows us to configure very large wells (up to 72 Me) for long integration times and low noise operation. The ROIC has a 1024x768 format and 20 µm pixel pitch.

At the time of LC6 material growth, we were not aware of the longer cut-off wavelengths in wafer lot runs. Although we suspected a longer cut-off wavelength, equally likely was that the doping calibration was off. Thus, we reduced the doping for this run by a factor of two. This material design has 97 quantum wells, so the loss of absorption from doping was compensated by the larger number of quantum wells. Figure 5 shows the measured spectrum of the test detector used for wafer acceptance and the spectrum of the FPA wafers. There was still a long shift to the cut-off wavelength, but since the cut-off slope of the test detector was not as sharp as it was for LC5, the shift was not as dramatic. The expected photoconductive gain is about the same as LC5, being near 0.17.

FPAs are currently being fabricated using LC6 wafers. The performance is expected to be very similar to the LC5 in terms of peak QE and NETD. The operating temperature is expected to rise and should be greater than 65K without using dark charge skimming.

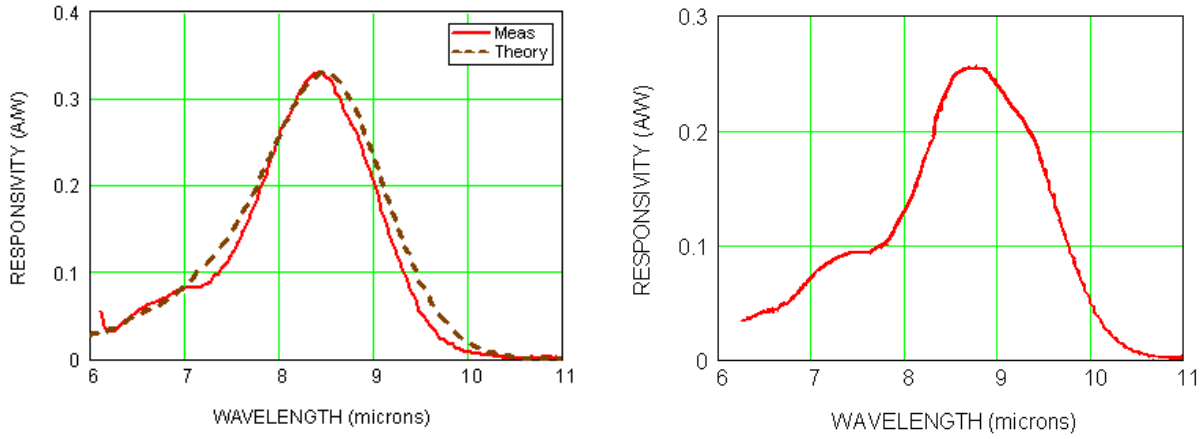

Figure 5: Acceptance detector spectrum (left) and FPA wafer spectrum (right) for LC6.

2.3. LC7 FPAs

We have one more LWIR tactical design currently in the wafer qualification stage that's designated LC7. LC7 will use our "lessons learned" from the LC5 and LC6 runs to create a true 9 µm cut-off with the higher doping of LC5 and the 97 quantum wells of LC6. The shorter cut-off wavelength and sharp cut-off slope should keep the operating temperature at the same level or higher than LC6. The increased doping and 97 quantum wells should establish the highest QE we can expect to achieve with the current detector geometry. A plot of the design spectrum for LC7 is shown in Figure 6.

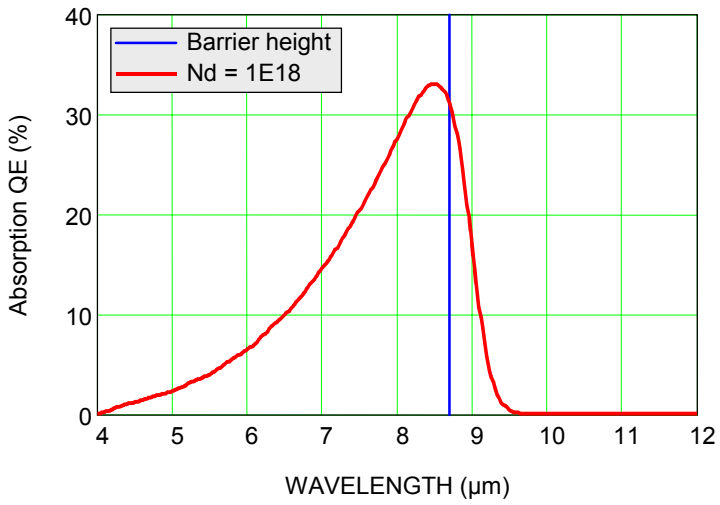

Figure 6: Design spectrum for the LC7 wafer.

3. TACTICAL TWO-COLOR FPAS

Spectral discrimination has been an effective means of target discrimination since the use of single element detectors in tactical systems. Spatially registered dual-band FPAs are of tactical interest because they integrate two sensors into one which reduces size, weight, and power requirements. Our current work is focusing on integrated MWIR and LWIR FPAs. The MWIR band is useful for long-range, high-resolution imagery. It is also useful against hot target events such as a MANPADS launch. The LWIR band is useful for high clutter backgrounds and small warm targets such as people and UAVs.

3.1. Dual-band C-QWIP Design

The dual-band C-QWIP uses a material design that detects one band when biased with positive voltage and the other band when biased with negative voltage. The structure consists of two-color unit cells separated by an energy relaxation barrier. A two-unit cell material design is shown in Figure 7. The unit cell consists of two superlattices of quantum wells. One superlattice is tuned to the MWIR band and the other to the LWIR band. In between the superlattices is a graded barrier. Under negative bias, photoelectrons generated in the second superlattice lose energy in the relaxation barrier and are blocked by the first superlattice. Under positive bias, the reverse situation occurs. This design creates complexity in the material growth, but does not alter the fabrication processes used for LWIR C-QWIPs.

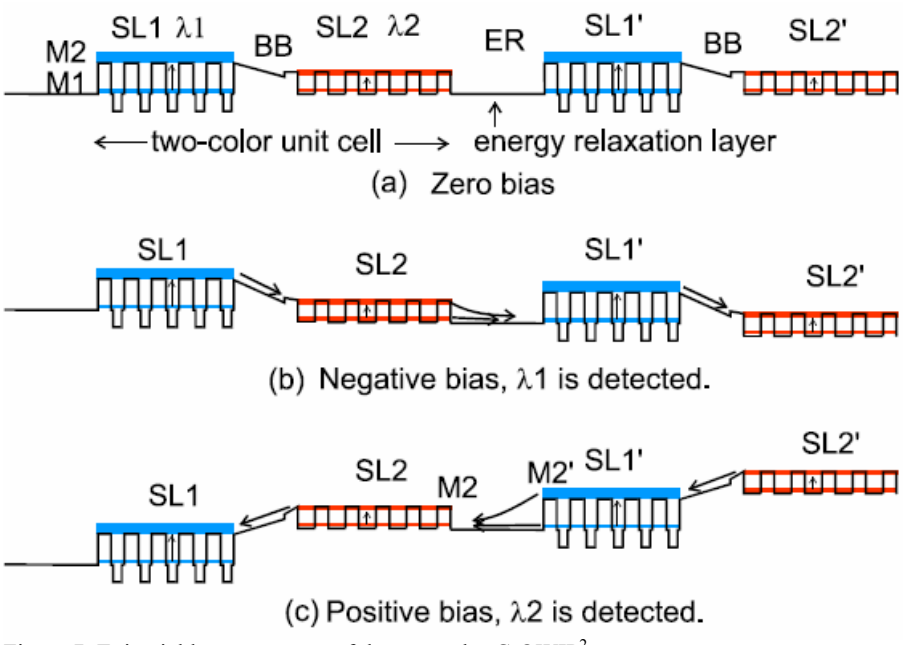

Figure 7: Epitaxial layer structure of the two-color C-QWIP[2].

Currently, we are performing wafer growth qualification on a perspective design. The spectrum for this design is shown in Figure 8. This design uses InGaAs quantum wells for the MWIR and GaAs quantum wells for the LWIR. This design is only a step towards a final design. After successful demonstration of an FPA using this design, we will focus on optimizing the absorption QE and spectral response.

3.2. Dual-band FPA Goals and Model Results

The performance goals for each band are basically the same as for the LWIR FPAs. We want to attain greater than 30% peak absorption QE in each band, have a bandwidth of 2 μm in the MWIR and 1.5 μm in the LWIR, and a photoconductive gain greater than 0.2. We actually expect the MWIR peak QE to be higher than the LWIR peak QE due to higher doping. The 2 μm bandwidth goal for the MWIR band is being deferred to a future material design.

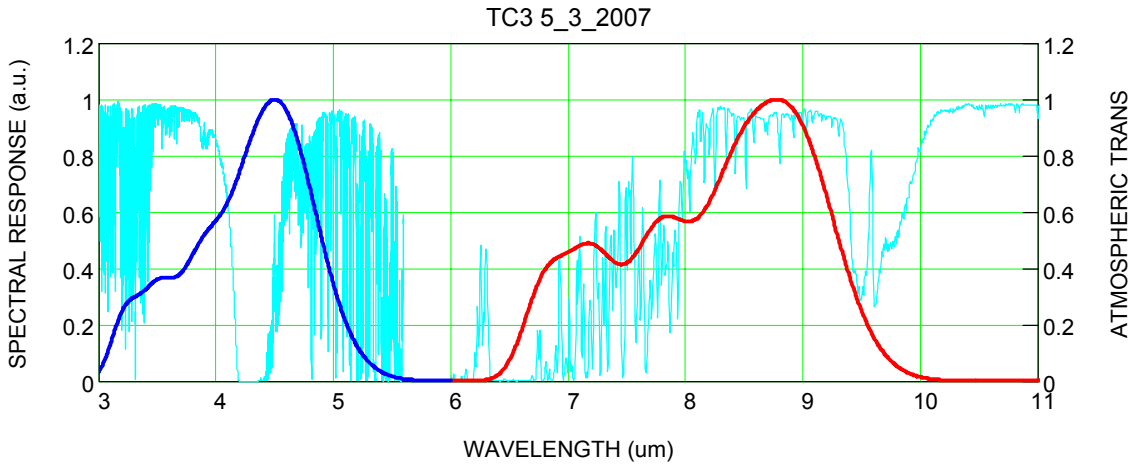

Figure 8: Spectrum of the dual-band material design currently being qualified for wafer growth.

Figure 9 shows the modeled spectral response of the dual-band material and a hypothetical atmospheric cold filter. This data is used within a camera model to determine the expected performance of this FPA. The photoconductive gain is assumed to be 0.2 for each band. We use an f/2.5 optic with an in-band transmission of 84%. The pixel fill factor is 80%, which is based on the current detector geometry. We assume the FPA is cooled such that the dark current is roughly 10% of the photocurrent at full well fill. The MWIR well size is set to 9 Me while the LWIR well size is set to 18 Me. The MWIR band integrates the maximum 20 milliseconds while the LWIR band integrates for 6.6 milliseconds. Under these conditions, we predict a NETD of 14.9 mK for the MWIR band and 16.3 for the LWIR band with a 300 K background. The predicted D* is 5.05×10^{12} Jones for the MWIR band and 6.11×10^{11} Jones for the LWIR band.

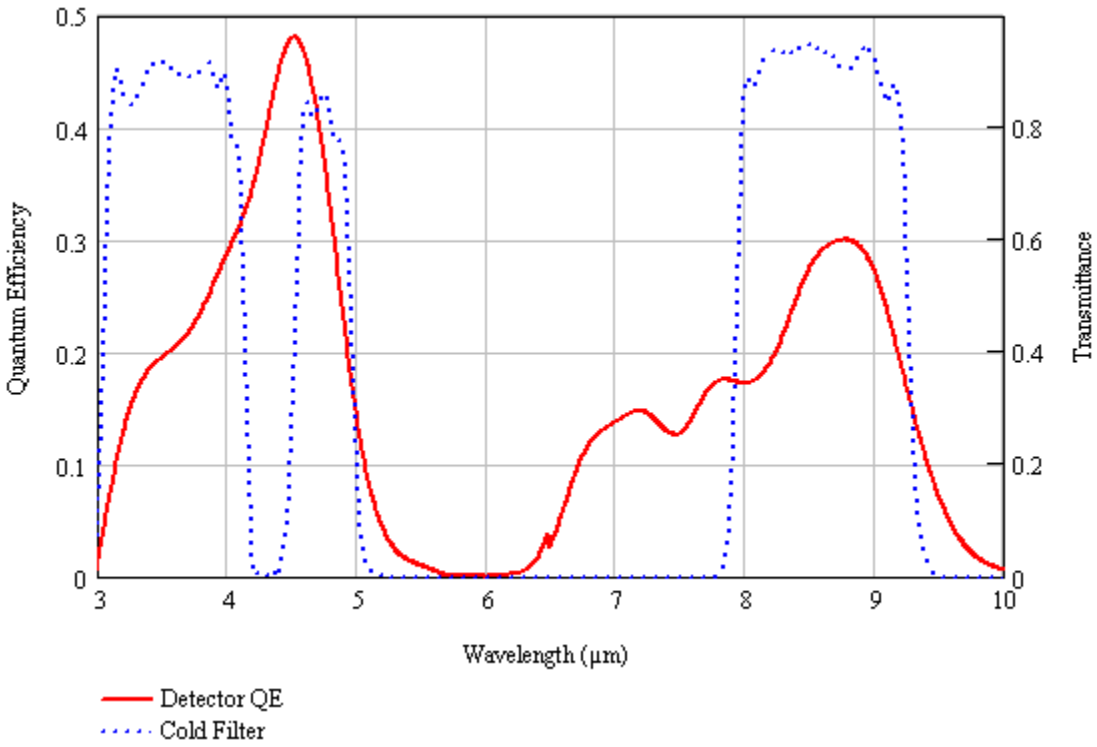

Figure 9: Simulated spectral response of the material and a hypothetical cold filter used for camera modeling.

4. FUTURE DEVELOPMENTS

4.1. Small Corrugations

Current pixel designs use a single set of micro-mirrors per pixel that we designate by "large corrugation". An alternate approach incorporates several pair's micro-mirrors as illustrated in Figure 10. There are two potential advantages to using small corrugations. First, the thickness of the quantum well material is much smaller. This reduces the growth time and increases photoconductive gain by reducing the transit time. Typically, we've measured photoconductive gains in the range of 0.2-0.3 for our large corrugation detectors. In a three corrugated structure, the expected photoconductive gain would be in the range of 0.6 to 0.9. This can reduce integration time, which is beneficial to certain tactical applications. The second advantage is a potential QE enhancement due to resonance. Simulations were performed[3] to investigate these potential resonant effects. The results are shown in Figure 11. For the usual level of doping in large corrugation pixels, the small corrugation pixels exhibit a minimum QE of 20% in the valleys with two peaks of 50% and 40% within the 8 to 10 μm band. The ε_i=1.0 curve in Figure 11 shows this absorption spectrum. This would yield a band average QE similar to that of a large corrugation pixel.

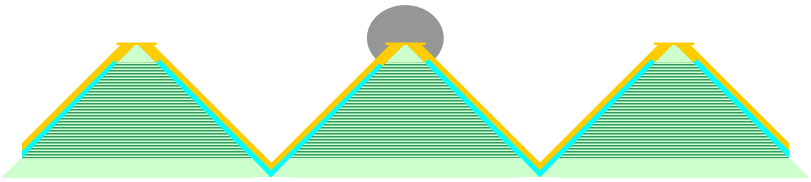

Figure 10: A small corrugation pixel with three sets of micro-mirrors.

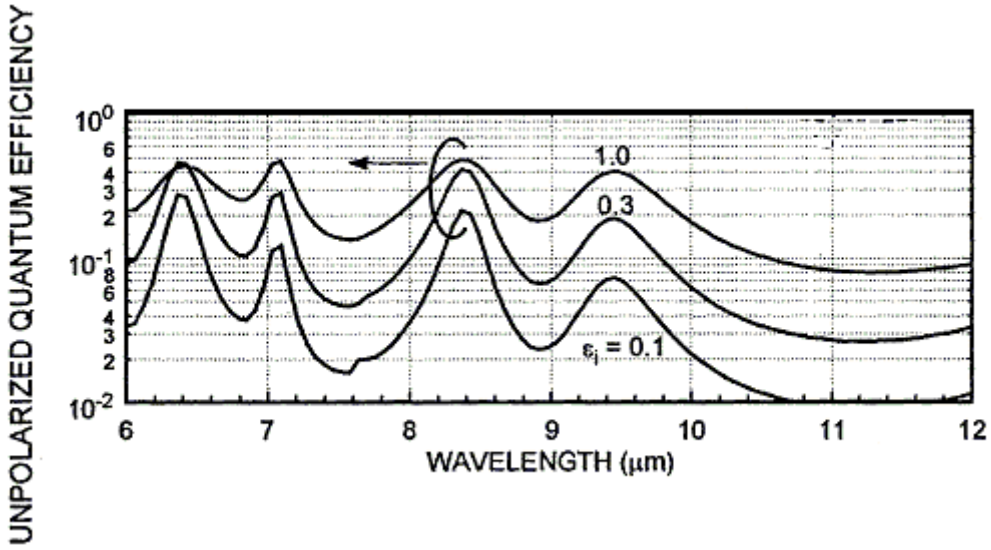

Figure 11: Simulation results of small corrugation C-QWIP resonance.

The modeling also suggests that as doping is decreased, the peak QE at the resonance can remain quite high. The ε_i=0.3 curve in Figure 11 shows how the peak absorption is nearly the same as the ε_i=1.0 curve, but the valley absorption is almost an order of magnitude lower. This feature can be useful for making multi-band or narrow band high operating temperature FPAs. One potential application is disturbed earth detection. In a recent paper[4], the apparent emissivity of soil increases greatly between 8.5 and 9.5 μm after the soil is disturbed, while in the band between 10.5 and 11.5 μm there is virtually no change. A small corrugation two-color C-QWIP design could provide significant discrimination between these two bands in an imaging sensor.

4.2. Corrugated Infrared Hot Electron Transistor (C-IHET)

The C-IHET is a single-band QWIP design that improves a QWIP's performance at low backgrounds and high f/#s. There are four sources that limit performance under these conditions. First, when an electron is elevated out of a quantum well by photon absorption, a positive charge is left in the well. Under high background illumination, this charge is quickly neutralized by dark current or recombining photoelectrons. At low backgrounds, the dark and photocurrents are much lower; therefore a space charge can accummulate that limits the bandwidth of the photoresponse. Second, the dominant noise source becomes 1/f noise from tunneling leakage currents because the noise from generation-recombination of dark current and photocurrent is small. Third, the dark current increases at low flux and high f/#s due to dark electron release from DX centers in the barriers. Finally, thermally assisted tunneling (TAT) dark current increases rapidly as the cut-off wavelength increases. This is due to low barrier heights. The additional TAT dark current requires the FPA to operate at even colder operating temperatures.

The C-IHET addresses these four problem sources in the following way. First, the barriers between the quantum wells in the QWIP are thin. Thin barriers increase ground state tunneling dark current, which neutralizes the charge left in the quantum wells. They also decrease the number DX centers in the barriers thus this additional source of dark current is reduced. Second, an energy barrier is placed between the QWIP and the output node. This barrier blocks the ground state tunneling and TAT dark currents while passing "hot" photoelectrons. By blocking these sources of dark current, the 1/f noise is greatly reduced. Finally, a node is placed between the QWIP and the barrier such that the tunneling dark current can drain to ground through that node. This three-node device forms a transistor where the QWIP detector common is the emitter, the node between the QWIP and the energy barrier is the base, and the output, which connects to the ROIC, is the collector.

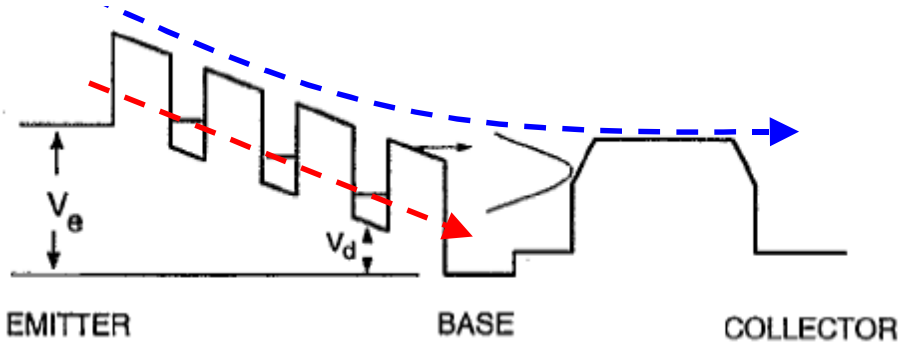

Figure 12: Band diagram of the infrared hot electron transistor.

Single device infrared hot electrons transistors (IHETs) have been demonstrated but never an FPA[5]. Our approach will fabricate a C-QWIP structure incorporating two common nodes and one pixel node. This structure is shown in Figure 13. This structure is more complicated to fabricate than a C-QWIP array but is easier to hybridize to the ROIC as there is only one contact per pixel.

In addition to improved performance under low flux conditions, the C-IHET offers additional advantages. One is that the QWIP bias voltage is completely contained to the GaAs substrate. This provides isolation between the QWIP and the ROIC. The bias voltage on the QWIP can exceed the voltage limitations of the ROIC without causing problems with the ROIC operation. Another is that the energy filter can reduce dark current in general and thus raise operating temperature. More elaborate energy filters can be designed. For example, a single detector IHET was designed[6] with a filter that blocked tunneling dark currents, passed photocurrent through high probability tunneling, and reduced thermionic dark current through low probability tunneling. This IHET increased photo to dark current ratio by an order of magnitude and allowed the FPA operating temperature to be raised.

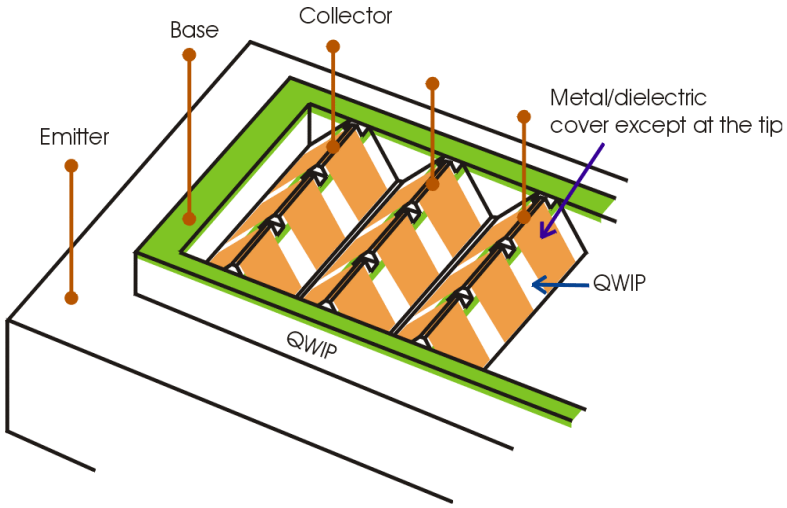

Figure 13: Proposed structure of a C-IHET FPA.

4.3. Ultra-large Format Two-Color FPA

CE was recently awarded a project to build a 2560×2560 format, 20 µm pitch MWIR FPA for persistent surveillance applications. The ROIC for this FPA is based upon our 1024x768 C-QWIP ROIC design such that we have the capability to fabricate, test, and package a 2560×2560 LWIR or two-color C-QWIP FPA.

4.4. Pyramidal Large Corrugated Pixels

The current C-QWIP pixels are tent-shaped structures. This structure provides efficient optical coupling in one direction and less efficient coupling in the other direction. By forming the micro-mirrors on all four sides of the pixel, as illustrated in Figure 14, efficient optical coupling can be obtained in both directions. This geometry decreases the detector cross section so the dark current decreases. Although the absorption path length decreases as well, the optical coupling is nearly doubled so the overall absorption QE increases. With the pyramidal C-QWIP, peak absorption QE around 50% should be feasible.

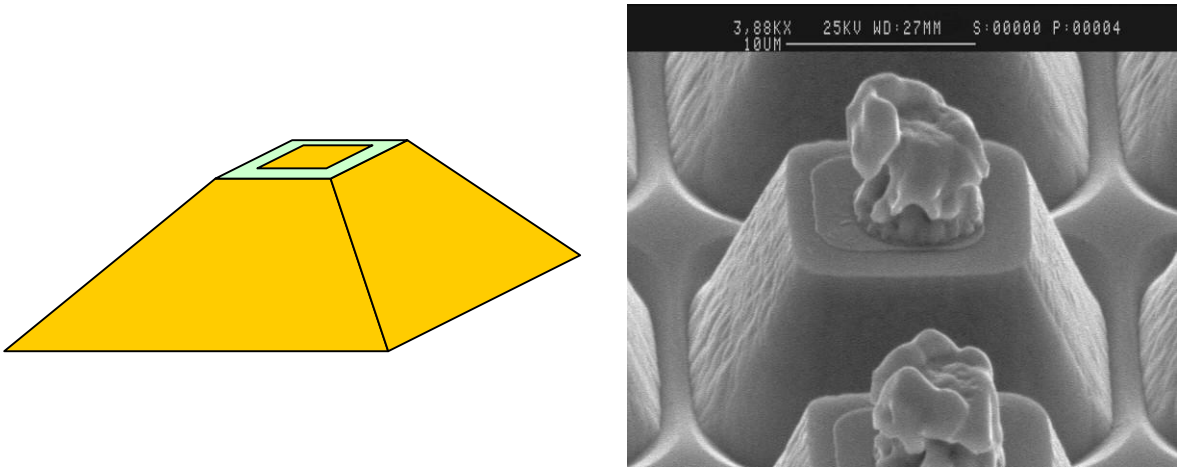

Figure 14: Illustration of pyramidal C-QWIP (left) and a SEM image of a test etch to create this geometry (right).

CONCLUSION

ARL and CE are continuing to develop the C-QWIP FPA technology to support tactical IR imaging applications. Much progress has been made on large format LWIR C-QWIP FPAs. These show much promise in providing wide area, high-resolution sensors at costs comparable to current MWIR products. The two most critical parameters for tactical

applications, integration time and NETD, are satisfied with our current material and detector designs. Small corrugations show promise of reducing integration time further by increasing the photoconductive gain and enhancing in-band absorption QE through resonance. The C-IHET potentially allows wider bandwidth, and thus more photocurrent, due to its ability to reduce dark current at longer cut-off wavelengths. The pyramidal structure also increases absorption QE through more efficient optical coupling with decreased dark current due to its smaller cross sectional area. All three of these approaches, alone or in combination, can further improve the performance of the tactical LWIR C-QWIP without adding substantial complexity to the FPA fabrication process.

Progress continues to be made on the dual-band material design. We are prepared to start fabrication of FPAs once the material design is finalized and grown into wafers. Small corrugation pixels show promise for creating dual-band or two-color FPAs with distinct spectral discrimination. Such FPAs may be useful in disturbed earth detection applications. The pyramidal pixels can also be used with dual-band and two-color FPAs without any changes to the material or hybridization process.

ARL and CE have highlighted their current progress toward high performance C-QWIP FPAs for LWIR and two-color tactical applications. In addition to the current work, future work in both the material design and pixel structure are identified, and show promise for further improving the performance of C-QWIPs in tactical systems.

REFERENCES

[1] K. K. Choi, J. W. Devitt, D. P. Forrai, D. Endres, J. Marquis, J. Bettge, P. Pinsukanjana, "C-QWIP material design and growth," SPIE DSS 2007

[2] K. K. Choi, C. Monroy, G. Dang, A. Goldberg, T. Tamir, K. M. Leung, M. Jhabvala, A. La, A. Majumdar, J. Li, D. C. Tsui, "Designs and Applications of Corrugated QWIPs", QWIP 2004

[3] K. K. Choi, K. M. Leung, T. Tamir, C. Monroy, "Light Coupling Characteristics of Corrugated Quantum-Well Infrared Photodetectors," IEEE JQE, Feb. 2004

[4] R. Harr and M. Polcha, "Preliminary Investigation of the Reststrahlen Phenomenology at Low-Grazing Angles," Proc. SPIE 2005

[5] C. Y. Lee, M. Z. Tidrow, K. K. Choi, W. H. Chang, L. F. Eastman, F. J. Towner, J. S. Ahearn, "Long-wavelength λ_c = 18 μm Infrared Hot Electron Transistor," J. Appl. Phys., May 1994

[6] C. Y. Lee, K. K. Choi, L. F. Eastman, "Infrared Hot-electron Transistor with a Narrow Bandpass Filter for High Temperature Operation," Appl. Phys. Lett., Jan. 1995